(Driving and) quenching of zonal flows on Gas Giants

Paula Wulff

University of California, Los Angeles
(work done at Max-Planck Institute for Solar System Research)

UCLA

Collaborators: Ulrich Christensen, Johannes Wicht, Wieland Dietrich, Vincent Böning

January 30, 2025

Contents

Contents

Zonal Winds on the Gas Giants

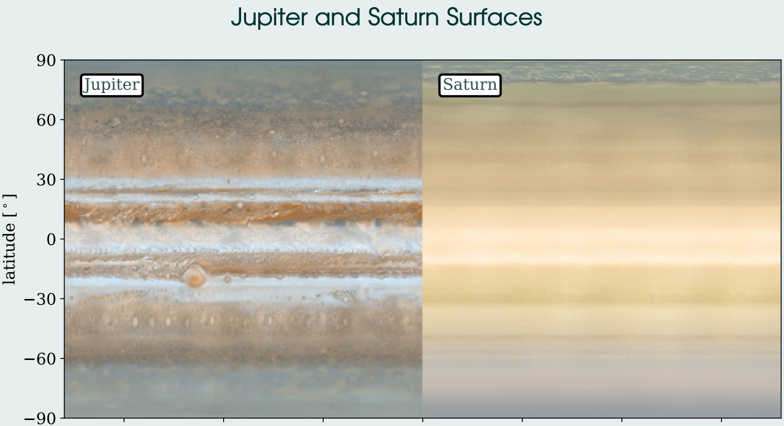

(source: Jupiter: NASA/JPL/Space Science Institute, Saturn: NASA/JPL)

Zonal Winds on the Gas Giants

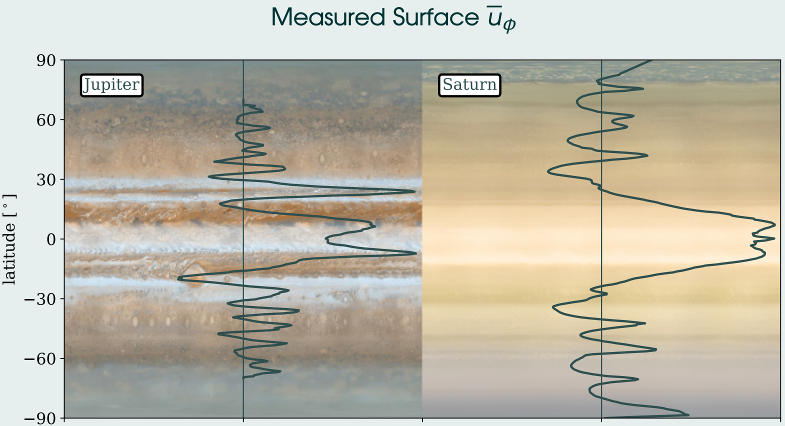

Jupiter: Tollefson et al. (2017). Saturn: García-Melendo et al. (2011), rot. period Mankovich et al. (2019).

Zonal Winds on the Gas Giants

Prograde/Superrotation/Eastward - Retrograde/Subrotation/Westward

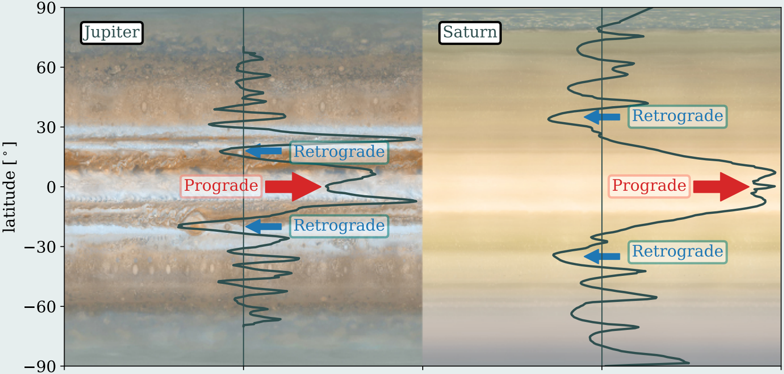

Jupiter: Tollefson et al. (2017). Saturn: García-Melendo et al. (2011), rot. period Mankovich et al. (2019).

Zonal Winds on the Gas Giants - Comparison

$$\overline{Ro_\phi} = \overline{u}_\phi / (\Omega r_o)$$

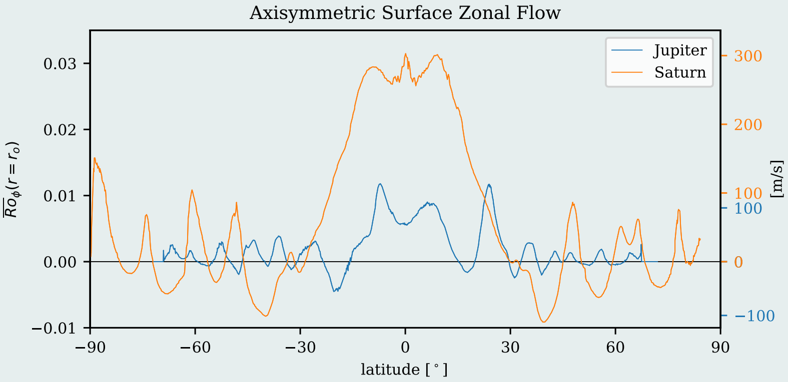

Jupiter: Tollefson et al. (2017). Saturn: García-Melendo et al. (2011), rot. period Mankovich et al. (2019).

Zonal Winds on the Gas Giants - Comparison

- Strong, broad equatorial prograde jet.
  - Jupiter: $\sim$ 120 m/s, spans $\pm 15^\circ$ longitude.
  - Saturn: $\sim$ 300 m/s, spans $\pm 30^\circ$ longitude.
- Flanking retrograde jets.
- Multiple jets at higher latitudes.
  - Jupiter: $\sim$ 30 m/s, narrower.
  - Saturn: $\sim$ 100 m/s, wider.

Zonal Winds on the Gas Giants - Depth

Measurement: Gravity Moments

- Measured *in-situ* for Jupiter (by Juno) and Saturn (by Cassini).
- Deep zonal winds have significant mass flux associated with them.

Assumptions

- Rotation dominates. Taylor-Proudman: zonal flow is geostrophic; z-invariant.
- Zonal flow decay is radially dependent.

Zonal Winds on the Gas Giants - Depth

Measurement: Gravity Moments

- Measured *in-situ* for Jupiter (by Juno) and Saturn (by Cassini).
- Deep zonal winds have significant mass flux associated with them.

Assumptions

- Rotation dominates. Taylor-Proudman: zonal flow is geostrophic; z-invariant.
- Zonal flow decay is radially dependent.

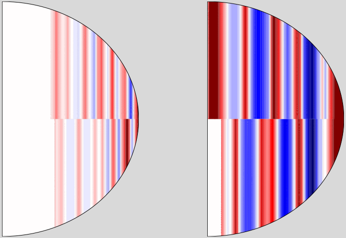

Zonal Winds on the Gas Giants - Depth

Measurement: Gravity Moments

- Measured *in-situ* for Jupiter (by Juno) and Saturn (by Cassini).
- Deep zonal winds have significant mass flux associated with them.

Assumptions

- Rotation dominates. Taylor-Proudman: zonal flow is geostrophic; z-invariant.
- Zonal flow decay is radially dependent.

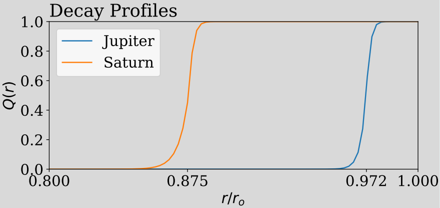

Zonal Winds on the Gas Giants - Depth

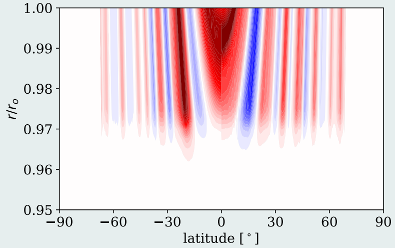

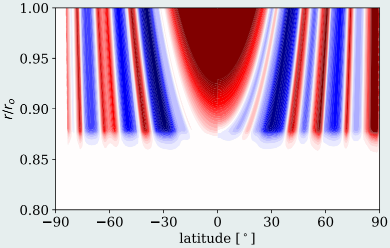

Jupiter: $\sim 2,500$ km, Saturn: $\sim 8,000$ km Galanti et al. (2020).

Question

How are the zonal winds truncated at depth?

Contents

Interior Structures of Jupiter and Saturn

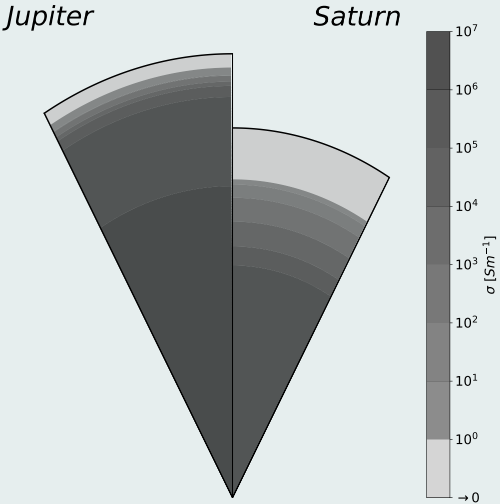

- Negligible conductivity in outer envelope (molecular hydrogen).
- Electrical conductivity increases sharply, yet smoothly, with depth.
- Highly conducting at depth (metallic hydrogen)

Jupiter: French et al. (2012), Saturn: Liu et al. (2008)

Interior Structures of Jupiter and Saturn

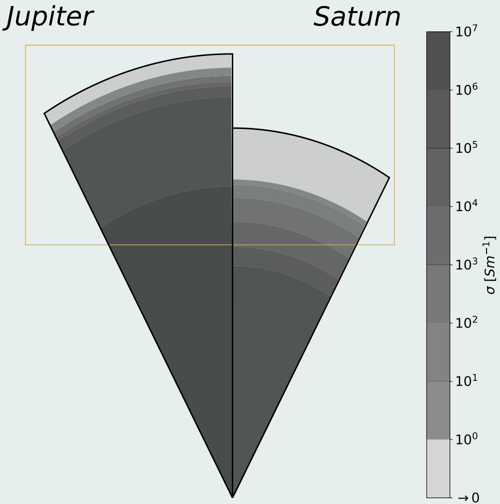

- Negligible conductivity in outer envelope (molecular hydrogen).
- Electrical conductivity increases sharply, yet smoothly, with depth.
- Highly conducting at depth (metallic hydrogen)

Jupiter: French et al. (2012), Saturn: Liu et al. (2008)

Interior Structures of Jupiter and Saturn

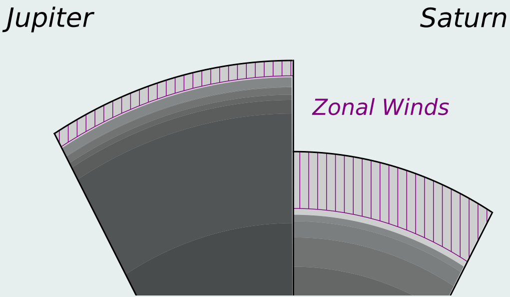

- Negligible conductivity in outer envelope (molecular hydrogen).
- Electrical conductivity increases sharply, yet smoothly, with depth.
- Highly conducting at depth (metallic hydrogen)

Consequences

Zonal winds restricted to non-conducting region.
Outer envelope fully convective - ?

Jupiter: French et al. (2012),
Saturn: Liu et al. (2008)

Contents

Hydrodynamic Models

Heimpel, Aurnou, Wicht (2005)

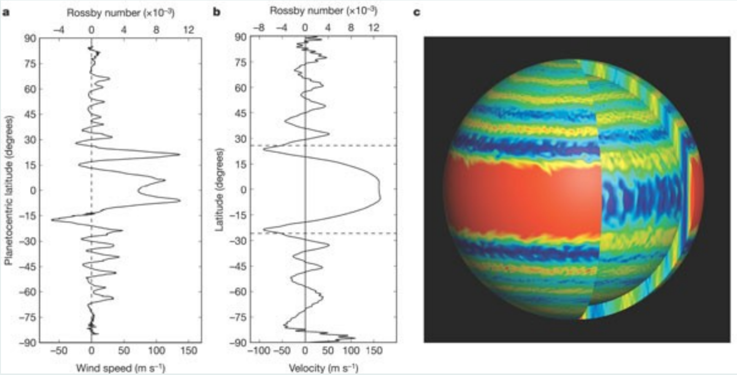

Thin, convecting shell with stress-free boundary conditions
→ multiple zonal jets

Hydrodynamic Models

Heimpel, Aurnou, Wicht (2005)

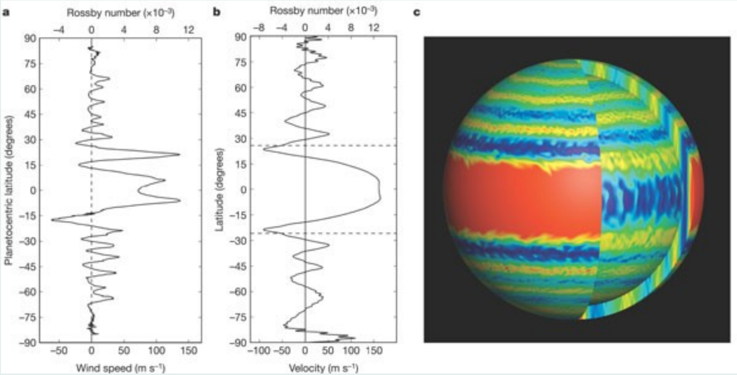

Thin, convecting shell with stress-free boundary conditions

→ multiple zonal jets ... but what quenches the winds at depth?

Partly Conducting Models

Heimpel and Gómez-Pérez (2011)

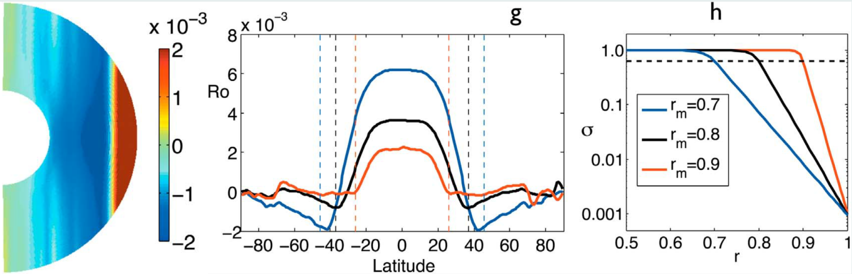

Sharp transition to high electrical conductivity
→ Equatorial jet

Partly Conducting Models

Heimpel and Gómez-Pérez (2011)

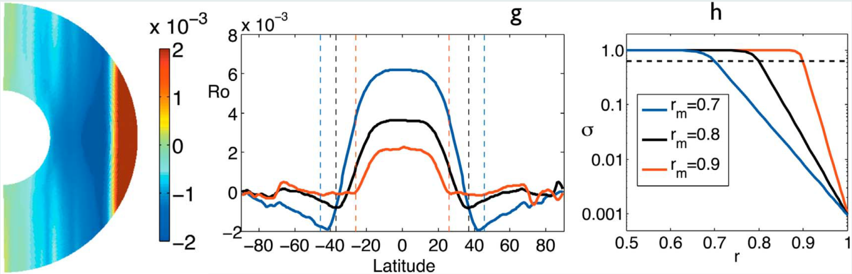

Sharp transition to high electrical conductivity

→ Equatorial jet ... but only weak flow inside magnetic tangent cylinder

Summary

Hydrodynamic models, with stress-free lower boundary:

- Mid-high latitude zonal winds ✓
- Zonal wind truncation mechanism ×

Magnetohydrodynamic models with increasing conductivity:

- Mid-high latitude zonal winds ×
- Zonal wind truncation mechanism ×

Summary

Hydrodynamic models, with stress-free lower boundary:

- Mid-high latitude zonal winds ✓
- Zonal wind truncation mechanism ×

Magnetohydrodynamic models with increasing conductivity:

- Mid-high latitude zonal winds ×
- Zonal wind truncation mechanism ×

Summary

Hydrodynamic models, with stress-free lower boundary:

- Mid-high latitude zonal winds ✓
- Zonal wind truncation mechanism ×

Magnetohydrodynamic models with increasing conductivity:

- Mid-high latitude zonal winds ×
- Zonal wind truncation mechanism ×

→ Proposal of Stably Stratified Layer (SSL): Christensen et al. (2020).

Contents

Governing Equations and Numerical Methods

- Mass Conservation
- Momentum Conservation (Navier-Stokes equation)
- Energy Equation
- Induction Equation

Code: `MagIC` (https://magic-sph.github.io/)

- Pseudo-spectral MHD code.
- Solves governing equations in rotating spherical shell.
- Uses anelastic or Boussinesq approximation.

Contents

Model Set-Up

Hydrodynamic Model

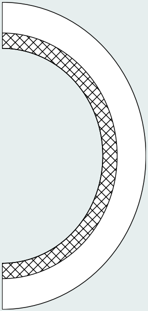

Outer 2/3 convecting.

Lower 1/3 stably stratified.

Rigid lower boundary condition.

Vary degree of stability

$$\rightarrow \frac{N}{\Omega} = \sqrt{\frac{Ra}{Pr}\tilde{g}\frac{dS_*}{dr}}E$$

N: Brunt Väisälä frequency

Model Set-Up

Hydrodynamic Model

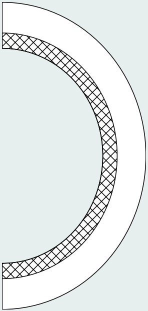

Outer 2/3 convecting.

Lower 1/3 stably stratified.

Rigid lower boundary condition.

Vary degree of stability

$$\rightarrow \frac{N}{\Omega} = \sqrt{\frac{Ra}{Pr}\tilde{g}\frac{dS_*}{dr}}E$$

N: Brunt Väisälä frequency

Magnetohydrodynamic Model

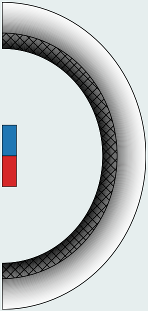

Outer 2/3 convecting.

Lower 1/3 stably stratified.

Exponentially increasing electrical conductivity.

Imposed axial dipole.

Vary electrical conductivity σ

Vary imposed field strength B_{dip}

$$\rightarrow \Lambda = \frac{B_{dip}^2 \sigma}{\tilde{\rho}\Omega}$$

Λ: Elsasser Number

Contents

Zonal Winds Formation

Prograde/Superrotation/Eastward - Retrograde/Subrotation/Westward

Reynolds Stresses

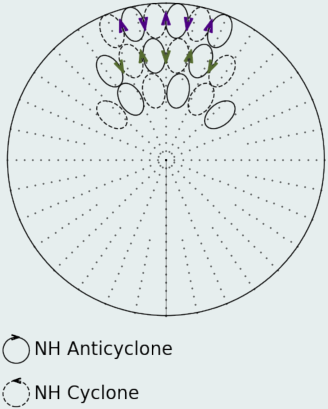

Zonal Winds Formation

Prograde/Superrotation/Eastward - Retrograde/Subrotation/Westward

Reynolds Stresses

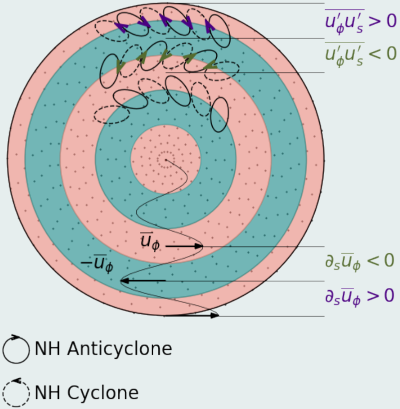

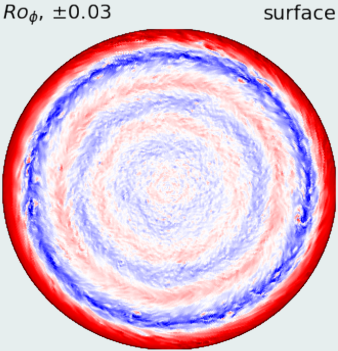

(simulation)

Zonal Winds Formation

Prograde/Superrotation/Eastward - Retrograde/Subrotation/Westward

Reynolds Stresses

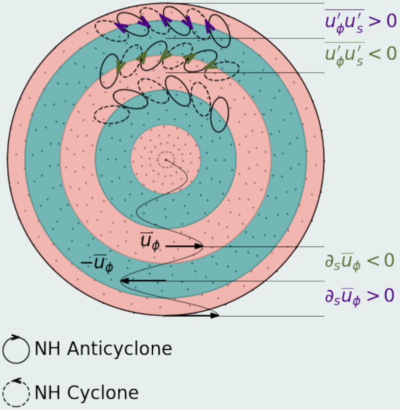

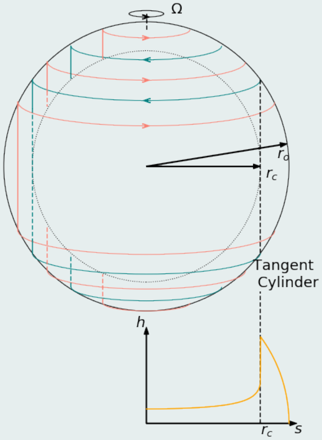

Zonal Winds in Simulations

Prograde/Superrotation/Eastward - Retrograde/Subrotation/Westward

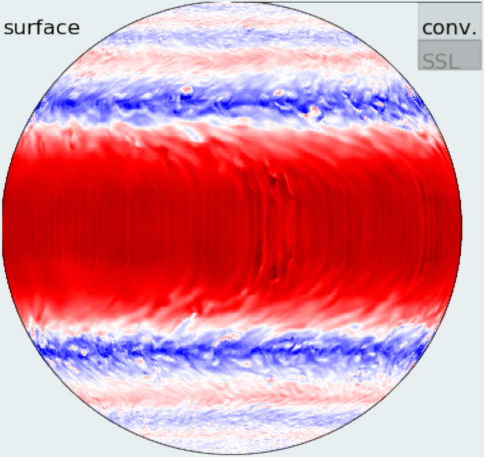

Zonal Winds in Simulations

Prograde/Superrotation/Eastward - Retrograde/Subrotation/Westward

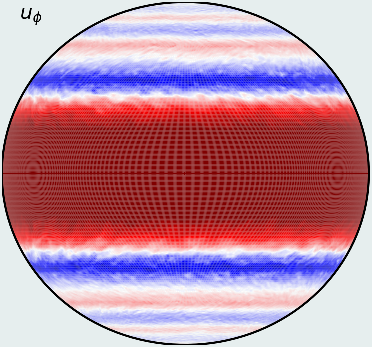

Zonal Winds in Simulations

Prograde/Superrotation/Eastward - Retrograde/Subrotation/Westward

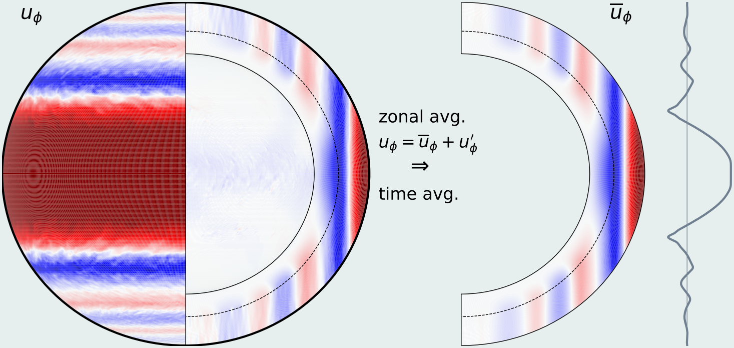

Hydrodynamic Study - Results

$\overline{Ro}_\phi$, colour-scale ± 0.03

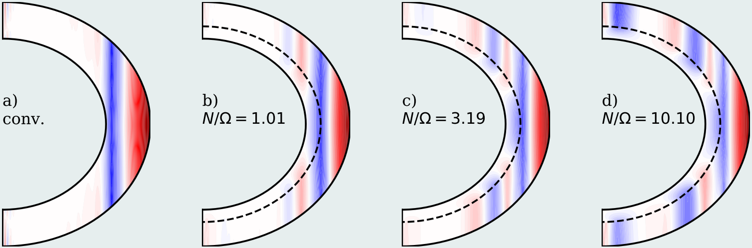

Higher degree of stability $\longrightarrow$ zonal winds at mid-high latitudes.

SSL decouples convective region from viscous forces below.

Hydrodynamic Study - Results

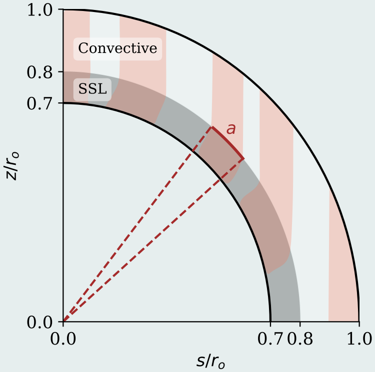

$$\delta(\overline{u}_\varphi^e) = \left|\frac{\partial \ln(\overline{u}_\varphi^e)}{\partial r}\right|^{-1}(r_c)$$

- Wider jets penetrate further into the SSL.
- Higher N/Ω; jets penetrate less deeply.

$$\delta(\overline{u}_\varphi^e) \propto \left(\frac{N}{\Omega}\right)^{-1} a$$

Hydrodynamic Study - Results

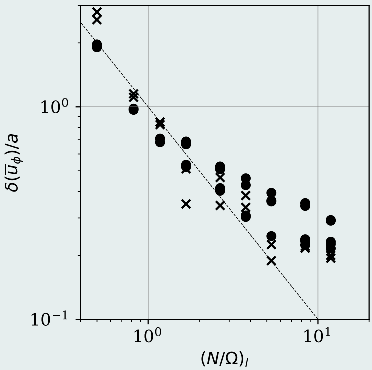

- Wider jets penetrate further into the SSL.
- Higher N/Ω; jets penetrate less deeply.

$$\delta(\overline{u}^e_\varphi) \propto \left(\frac{N}{\Omega}\right)^{-1} a$$

Magnetohydrodynamic Study - Surface Winds

$\overline{Ro_{\phi}}$, colour-scale ± 0.018

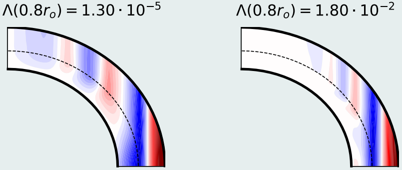

Weak magnetic field strength, weakly conducting at SSL boundary
$\longrightarrow$ zonal winds at mid-high latitudes.

Magnetohydrodynamic Study - Surface Winds

$\overline{Ro_\phi}$, colour-scale ± 0.018

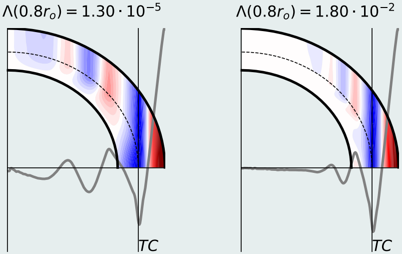

Weak magnetic field strength, weakly conducting at SSL boundary
$\rightarrow$ zonal winds at mid-high latitudes.

Magnetohydrodynamic Study - Surface Winds

$\overline{Ro}_\phi$, colour-scale ± 0.018

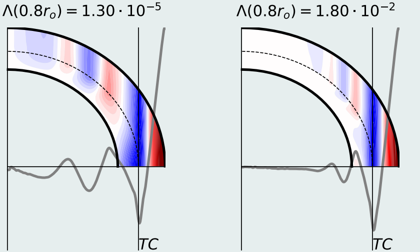

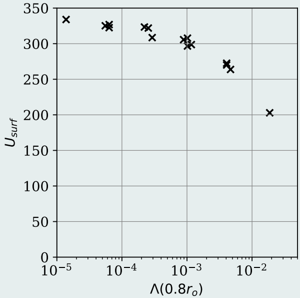

Weak magnetic field strength, weakly conducting at SSL boundary
$\rightarrow$ zonal winds at mid-high latitudes.
SSL decouples convective region from magnetic forces below.
Low Λ at r_c, zonal winds tend to same structure in convective envelope.

Magnetohydrodynamic Study - Winds at Depth

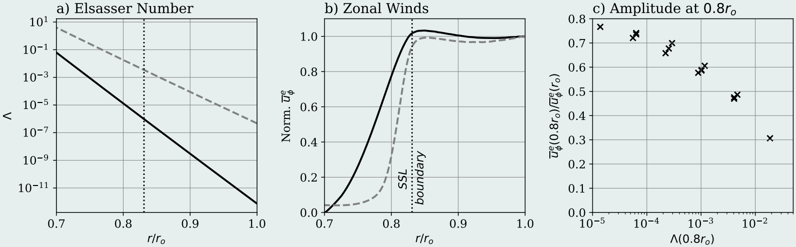

Truncation Mechanism - Thermal Wind

Vorticity Conservation (azimuthal component of curled N-S eq.):

$$0 = 2\partial_z\langle\overline{u}_\phi\rangle - \frac{RaE}{Pr}\frac{\tilde{g}}{r}\partial_\vartheta\langle\bar{s}_c\rangle + \dots \qquad \langle\cdot\rangle : \text{time avg.}$$

Thermal Wind Balance:

$$2\partial_z\langle\overline{u}_\phi\rangle \approx \frac{RaE}{Pr}\frac{\tilde{g}}{r}\partial_\vartheta\langle\bar{s}_c\rangle.$$

Vertical variation of Zonal flow velocity $\leftrightarrow$ *Latitudinal temperature (entropy) variations*

Truncation Mechanism - Thermal Wind

Thermal Wind Balance:

$$2\partial_z\langle\overline{u}_\phi\rangle \approx \frac{RaE}{Pr}\frac{\tilde{g}}{r}\partial_\vartheta\langle\bar{s}_c\rangle.$$

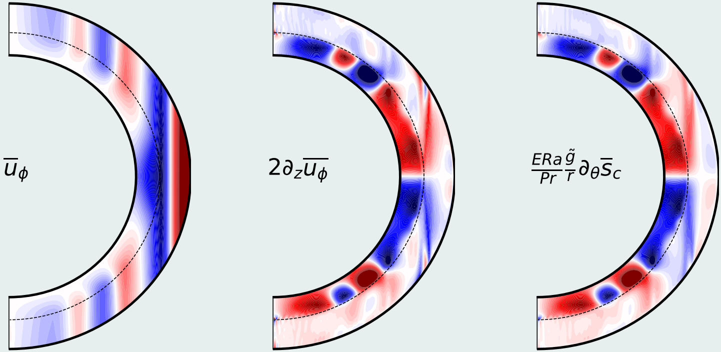

Truncation Mechanism - Thermal Wind

Insights

Near perfectly geostrophic (z-invariant) in convective region.
Latitudinal temperature variations lead to zonal wind quenching.

Question

What causes the meridional circulation leading to the temperature structure alteration?

Truncation Mechanism - Forces

Zonal Force Balance: $0 = \langle \overline{F}_{Ad} \rangle + \langle \overline{F}_{C} \rangle + \langle \overline{F}_{R} \rangle + \langle \overline{F}_{Ma} \rangle + \langle \overline{F}_{Mna} \rangle + \langle \overline{F}_{\nu} \rangle$

$$
\begin{aligned}
\overline{F}_{Ad} &= \frac{\overline{u}_s}{s}\partial_s(s\overline{u}_\phi) + \overline{u}_z\partial_z(\overline{u}_\phi) \\
\overline{F}_{C} &= \frac{2}{E}\overline{u}_s \\
\overline{F}_{R} &= \frac{1}{s^2}\partial_s\left[s^2\overline{u_s' u_\phi'}\right] + \partial_z\left[\overline{u_z' u_\phi'}\right] \\
\overline{F}_{Ma} &= \frac{-1}{EPm}\left[\frac{1}{s^2}\partial_s\left(s^2\overline{B_\phi}\,\overline{B_s}\right) + \partial_z\left(\overline{B_\phi}\,\overline{B_z}\right)\right] \\
\overline{F}_{Mna} &= \frac{-1}{EPm}\left[\frac{1}{s^2}\partial_s\left(s^2\overline{B_\phi' B_s'}\right) + \partial_z\left(\overline{B_\phi' B_z'}\right)\right] \\
\overline{F}_{\nu} &= -\frac{1}{s^2}\partial_s\left[s^3\partial_s\left(\frac{\overline{u}_\phi}{s}\right)\right] - \partial_z\left[\partial_z\left(\overline{u}_\phi\right)\right].
\end{aligned}
$$

Reduced Zonal Force Balance: $0 \approx \langle \overline{F}_{C} \rangle + \langle \overline{F}_{R} \rangle + \langle \overline{F}_{Ma} \rangle$

Coriolis, Reynolds Stresses, Large-scale Maxwell Stresses

Truncation Mechanism - Forces

Coriolis Force

Reynolds stress divergence

Lorentz Forces

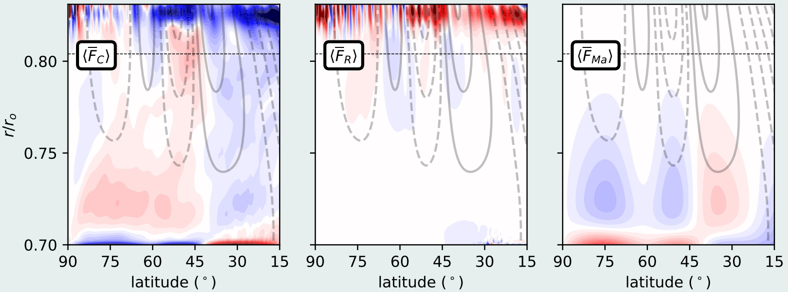

Coriolis Force

Reynolds stress divergence

Lorentz Forces

Truncation Mechanism - Forces

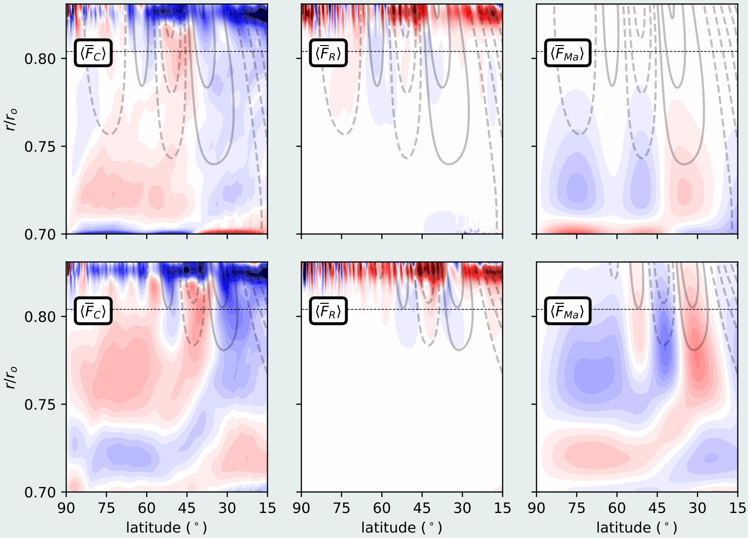

Contents

Governing Equations

$$\frac{\partial \boldsymbol{u}}{\partial t} + (\boldsymbol{u} \cdot \nabla)\boldsymbol{u} = -\nabla P - 2\boldsymbol{\Omega} \times \boldsymbol{u} + \boldsymbol{F}_{\nu} + \frac{\boldsymbol{J} \times \boldsymbol{B}}{\tilde{\rho}} + C\boldsymbol{g}$$

$$\frac{\partial \boldsymbol{B}}{\partial t} = \nabla \times (\boldsymbol{u} \times \boldsymbol{B}) - \nabla \times (\frac{1}{\mu_0 \sigma} \nabla \times \boldsymbol{B})$$

$$\frac{\partial C}{\partial t} + \boldsymbol{u} \cdot \nabla C = \frac{1}{\tilde{\rho}} \nabla \cdot (\kappa \tilde{\rho} \nabla C)$$

$$\nabla \cdot (\tilde{\rho} \boldsymbol{u}) = 0, \qquad \nabla \cdot \boldsymbol{B} = 0$$

Set-up and Non-dimensionalisation

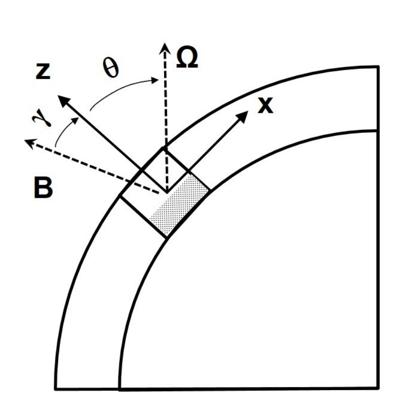

- Consider only stable layer $z < 0$
- Zonal flow: $U = u_y$
- Meridional stream function: $\boldsymbol{u} = \nabla \times \Psi \boldsymbol{e}_y$
- Induced toroidal magnetic field: $b = B_y$
- codensity perturbation: c
- Neglect all non linear terms, viscosity, poloidal field perturbations. Set $\partial/\partial t = 0$.
- Harmonic variation $\sim \exp(ikx)$ of U, Ψ, b, c

Set-up and Non-dimensionalisation

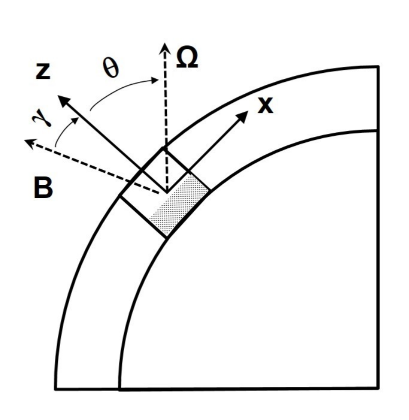

Scaling:

- $U = \tilde{U}\kappa/d_\sigma$
- $\Psi = \tilde{\Psi}\frac{\kappa\sigma_o B^2}{\rho_o \Omega}$
- $b = \tilde{b}\kappa\sigma_o\mu_o B$
- $c = \tilde{c}\frac{\sigma_o d_\sigma B^2 N^2}{\rho_o g \Omega}$

Simplified Equations

$$2d_z\Psi = -d_z b$$

$$d_z U = MAC\,kc$$

$$(d_{zz} - k^2)c = -k\Psi$$

$$(d_{zz} + d_z - k^2)b = -\exp(-z)d_z U$$

Simplified Equations

$$2d_z\Psi = -d_z b$$

$$d_z U = MAC\, kc$$

$$(d_{zz} - k^2)c = -k\Psi$$

$$(d_{zz} + d_z - k^2)b = -\exp(-z) d_z U$$

$$MAC = \left(\frac{N}{\Omega}\right)^2 \frac{\sigma_o B^2 d_\sigma^2}{2\rho_o \kappa}$$

Balance of

Magnetic: $\Lambda = \frac{\sigma_o B^2}{\rho_o \Omega}$

Archimedean: N/Ω

Coriolis: $E_\kappa = \frac{\kappa}{d_\sigma^2 \Omega}$

Contents

Variation with stable layer depth

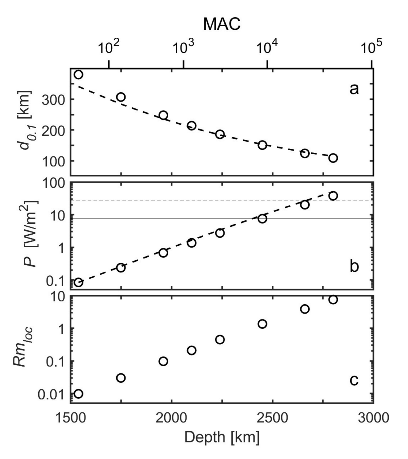

Jupiter-like case at **mid-latitude** as function of the depth of the stable layer boundary for a wind velocity of **25 m/s**, characteristic latitudinal wavelength of the zonal jets inside the tangent cylinder **10,000 km**, stability $\boldsymbol{N/\Omega = 1}$.

a) Decay range $d_{0.1}$,

b) driving power,

c) maximum value of the local magnetic Reynolds number.

Variation with stable layer depth

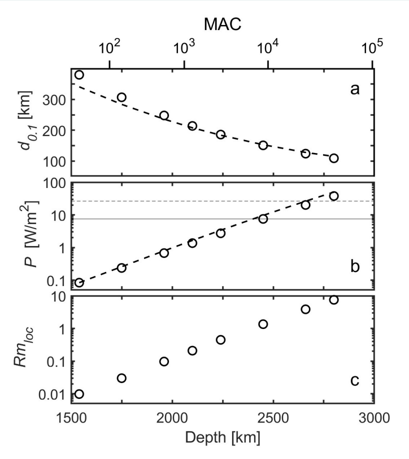

a)
Jet velocity drops tenfold over a depth of 100-300 km.
At lower MAC (shallower stable layer boundary) winds penetrate deeper into the stable layer.

Variation with stable layer depth

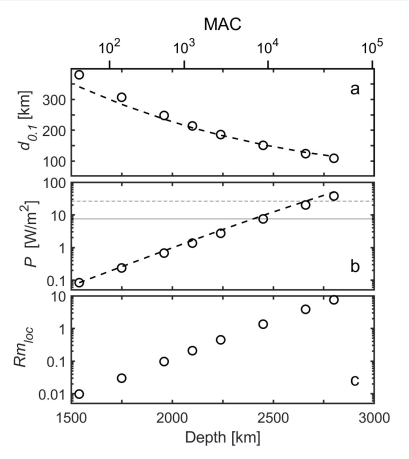

b)

The thin full line is the observed internal heat flow and the broken line is the upper bound for the total dissipative heating according to Wicht+ (2019).

It is unlikely that the dissipation linked to the zonal winds substantially exceeds the internal heat flow.

This would be the case if the stable layer boundary was deeper than 2,500 km

Variation with stable layer depth

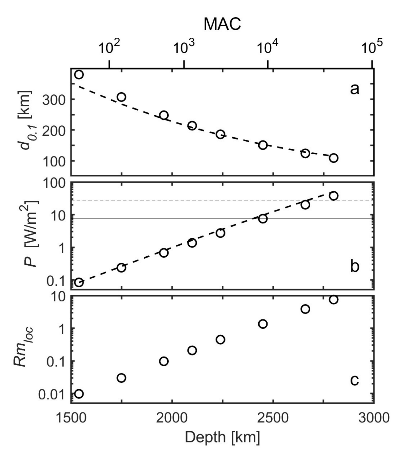

c)

A large magnetic reynolds number would perturb the poloidal magnetic field. Such distortions are not observed. Taking $Rm_{loc} = 3$ as an upper limit requires the stable layer boundary to be no deeper than 2,600 km
$\rightarrow$ almost identical to the constraint based on the driving power.

Variation with latitude

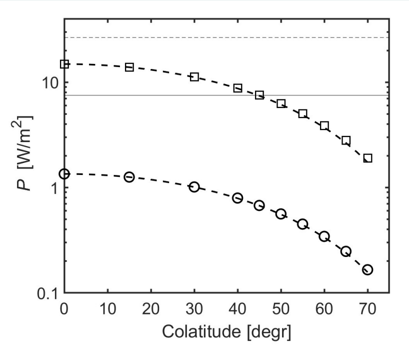

Insignificant variation of $d_{0.1}$ with colatitude.
Variation of power was found to be mainly due to change in angle between gravity and magnetic field.

Contents

Summary

- A Stably stratified Layer (SSL) does not prevent strong zonal winds from forming in overlying convective envelope.
- SSL's lead to the decay of zonal flows penetrating down from a convective region, controlled by the MAC number.
- A thermal wind balance governs the attenuation of zonal flows in the SSL.

Summary - Shallow Stable Layer

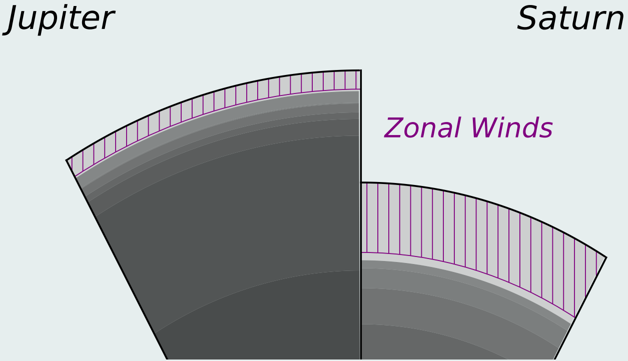

Summary - Shallow Stable Layer

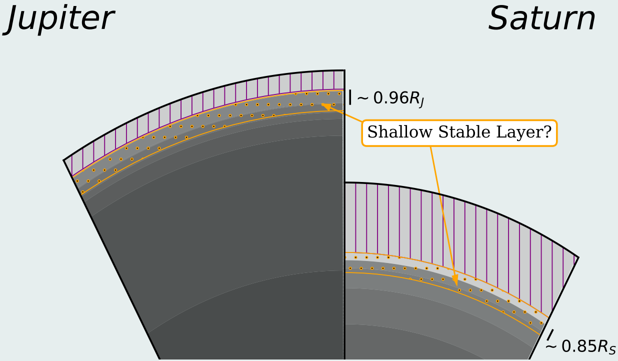

Summary - Shallow Stable Layer

Conclusion

For mid-high latitude jets to form on Jupiter and Saturn a Stably Stratified Layer must be located where jet quenching begins, above highly electrically conducting depths.

References

- J. Tollefson, M. H. Wong, I. de Pater, A. A. Simon, G. S. Orton, J. H. Rogers, S. K. Atreya, R. G. Cosentino, W. Januszewski, R. Morales-Juberías, P. S. Marcus.
  Changes in Jupiter's Zonal Wind Profile preceding and during the Juno mission.
  Icarus. 2017.
- E. García-Melendo, S. Pérez-Hoyos, A. Sánchez-Lavega, R. Hueso.
  Saturn's zonal wind profile in 2004-2009 from Cassini ISS images and its long-term variability.
  Icarus. 2011.
- C. Mankovich, M. S. Marley, J. J. Fortney, N. Movshovitz.
  Cassini Ring Seismology as a Probe of Saturn's Interior. I. Rigid Rotation.
  The Astrophysical Journal. 2019.

References

- E. Galanti, Y. Kaspi.
  Combined magnetic and gravity measurements probe the deep zonal flows of the gas giants.
  Monthly Notices of the Royal Astronomical Society. 2020.
- M. French, A. Becker, W. Lorenzen, N. Nettelmann, M. Bethkenhagen, J. Wicht, R. Redmer.
  Ab Initio Simulations for Material Properties along the Jupiter Adiabat.
  The Astrophysical Journal Supplement Series. 2012.
- J. Liu, P. Goldreich, D. Stevenson.
  Constraints on deep-seated zonal winds inside Jupiter and Saturn.
  Icarus. 2008.

References

M. Heimpel, J. Aurnou, J. Wicht.
Simulation of equatorial and high-latitude jets on Jupiter in a deep convection model.
Nature. 2005.

M. Heimpel, N. Gómez-Pérez.
On the relationship between zonal jets and dynamo action in giant planets.
Geophysical Research Letters. 2011.

U. R. Christensen, J. Wicht, W. Dietrich.
Mechanisms for Limiting the Depth of Zonal Winds in the Gas Giant Planets.
The Astrophysical Journal. 2020.

References

P. N. Wulff, W. Dietrich, U. R. Christensen, J. Wicht.
Zonal winds in the gas planets driven by convection above a stably stratified layer.
Monthly Notices of the Royal Astronomical Society. 2022.

P. N. Wulff, U. R. Christensen, W. Dietrich, J. Wicht.
The Effects of a Stably Stratified Region With Radially Varying Electrical Conductivity on the Formation of Zonal Winds on Gas Planets.
JGR - Planets. 2024.